Applied Surface Science 28 (1987) 331–344
North-Holland, Amsterdam

THE ELECTROCHEMISTRY OF InP IN Br_2/HBr SOLUTIONS AND ITS RELEVANCE TO ETCHING BEHAVIOUR

P.H.L. NOTTEN and A.A.J.M. DAMEN

Philips Research Laboratories, P.O. Box 80.000, 5600 JA Eindhoven, The Netherlands

Received 2 March 1987; accepted for publication 6 April 1987

Etch rate–potential curves of p-InP in HBr and Br_2/HBr solutions in the dark and under illumination were correlated with current–potential curves. It was found that InP is etched via a "chemical" mechanism both by HBr and Br_2. In aqueous HBr solutions InP is only etched at a significant rate at concentrations higher than 5 mol/ℓ. The Br_2 etchants contained 4.5M HBr; in this case HBr only serves to complex Br_2 to Br_3^-. The etch rate in Br_2/HBr solutions is mass-transport controlled at InP(001) and kinetically controlled at InP with the (111) In orientation. The macroscopically obtained results are consistent with the profiles etched at resist edges in InP. The electrochemistry of Br_2 at p-InP under illumination reveals some interesting aspects with regard to the agreement between the etch rate and the Br_2 reduction.

1. Introduction

InP single crystals are important in the fabrication of opto-electronic devices. Etching plays an essential role in the production of these devices. Various etching baths including bromine solutions are described in the literature [1,2]. Bromine solutions can be divided into organic, for instance Br_2 in methanol [3], and aqueous solutions [4]. In the present paper we consider only aqueous bromine solutions.

Br_2 cannot be dissolved easily in water. Moreover, the partial vapour pressure of bromine is large which results in a rapid decrease of the bromine concentration in the solution as a function of time. To overcome this problem Br_2 can be complexed in bromide solutions to Br_3^- and Br_5^- respectively according to

$$Br_2 + Br^- \rightleftarrows Br_3^- , \quad (1)$$

$$2\ Br_2 + Br^- \rightleftarrows Br_5^- . \quad (2)$$

From the equilibrium constants, 0.051 and 0.0246 for eq. (1) and eq. (2), respectively [5], it is calculated that Br_2 is complexed almost completely to Br_3^- when a large excess of Br^- is available. In the present work we complexed Br_2 in acid HBr solutions.

In recent work we and other authors have shown that the shape of the etched profiles, obtained at semiconductor crystals covered with semi-infinite masks, depends strongly on the etching mechanism, either electrochemical or chemical, and etching kinetics [6–8]. To clarify both the mechanism and kinetics flow-cell experiments were performed under potentiostatic control at p-InP in Br_2/HBr solutions, in the dark and under illumination. It is known, however, that InP can also be etched in solutions of HBr [4,9]. To elucidate the contribution of HBr to the dissolution rate of InP we first examined the etching mechanism and kinetics of InP in HBr solutions.

Finally, etching experiments were done to show that macroscopically measured etch rates are consistent with the etch rates obtained at etched profiles on a microscopic scale.

2. Experimental

The p-type InP wafers used in this work were obtained from liquid-encapsulated Czochralski material with a carrier density in the range $(1-2) \times 10^{18}$ cm^{-3}. In almost all cases the (001) face was exposed to the solution. In one etching experiment we used the (111) In face of the InP crystal.

The current–potential measurements were carried out in either a conventional gas-closed electrochemical cell or a micro-electrochemical flow-cell using a Pt counter electrode and a saturated calomel electrode (SCE) as reference. All potentials are given with respect to this SCE. The working electrode was illuminated with a 150 W Schott halogen lamp (KL 150 B) in combination with a glass fibre light cable.

The dissolution rate of InP at a fixed potential was determined analytically by measuring the indium concentration in the electrolyte by induced-coupled plasma (ICP) emission spectrometry. The electrode was mounted in a micro-electrochemical flow-cell as described by Haroutiounian et al. [10]. The solution was pumped over the electrode with an LKB varioperpex peristaltic pump. The flow rate of the solution, mainly determined by the lower limit of the indium detection, was in the range of 0.14 to 1.62 ml/min.

The etching experiments were performed in a closed glass vessel with InP crystals of (001) orientation. The surface was partly covered with an SiO_2 mask. The thickness of the mask was about 0.1 μm. The SiO_2 resist edge was aligned in the $(\bar{1}10)$ direction. The InP crystals were mounted on a glass plate and placed horizontally in the etching solution. After etching, the crystal was cleaved perpendicular to the SiO_2 windows and the cleaved face was examined in a scanning electron microscope (SEM).

All solutions were prepared from reagent grade concentrated solutions: acetic acid (100%); hydrobromic acid (47%, ~ 9 molar) and bromine (100%, ~ 20 molar) and were supplied by Merck.

All measurements were performed at room temperature unless otherwise stated.

3. Results

3.1. HBr solutions

In the flow-cell experiments of fig. 1 the etch rate of InP(001) in the dark at open circuit potential is shown as a function of the HBr concentration. The concentration of HBr was varied over a wide range by diluting the concentrated HBr stock solution with water (curve (a)). The dissolution rate of InP is very low for concentrations up to 5 molar. The etch rate at concentrations higher than 5 molar increases rapidly with increasing HBr concentration and gas evolution is observed. For curve (b) the HBr concentration was varied by diluting the stock solution with concentrated acetic acid. The etch rate depends linearly on the HBr concentration and is much higher than that of HBr/H_2O solutions.

The influence of the anodic dissolution behaviour of p-InP(001) was studied potentiodynamically in fig. 2 in various solutions. In 1N H_2SO_4 (curve (a)) the dissolution starts near the flat-bland potential and increases exponentially at positive potentials as expected for a p-type electrode. In 4.5N HBr (curve (b))

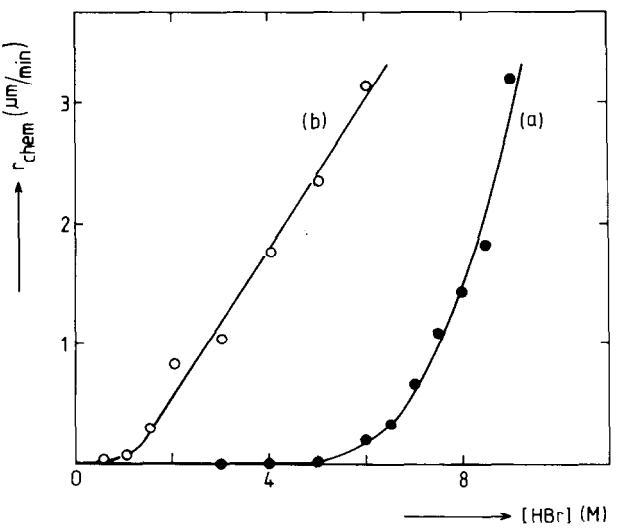

Fig. 1. Chemical etch rate as a function of the HBr concentration for a p-InP(001) crystal in the dark. The HBr concentration was varied by diluting the stock solution with water (curve (a)) and concentrated acetic acid (curve (b)).

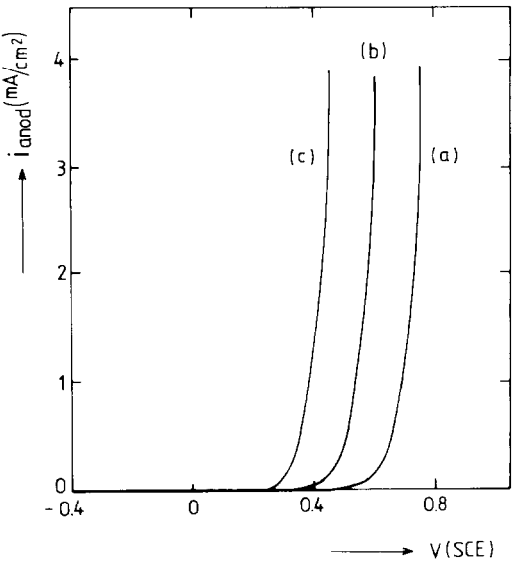

Fig. 2. Current–potential curves for a p-InP electrode in the dark in 0.5M H_2SO_4 (a), 4.5M HBr (b) and 0.1M Br_2 in 4.5M HBr (c). The scan rate was 50 mV/s.

the anodic dissolution starts earlier. The dissolution curve is here shifted by about 150 mV to negative potentials.

3.2. Br_2/HBr solutions

The flow-cell experiments of fig. 3 show the potentiostatically measured current densities (curve (a)) and etch rates (curve (b)) of a p-InP electrode in the dark in 0.1M Br_2 and 4.5M HBr solution. The etch rates are expressed as a current density assuming that six holes are needed to dissolve one InP entity. At negative potentials the current density is low. The anodic dissolution starts at 0.2 V, a rather negative potential with respect to the flat-band potential ($V_{fb} = 0.73$ V [11]), and increases at more positive potentials. In the potential range where no current is observed, InP is etched at a considerable rate (curve (b)). The etch rate is independent of the applied potential. This behaviour is typical of a chemical etchant as was found before for InP [11] and GaAs [12,13]. In the potential range where an anodic current is observed the etch rate increases; in addition to chemical etching, anodic dissolution of InP occurs in this range.

In the potentiodynamically measured current–potential curve of fig. 2 (curve (c)) in a solution of Br_2/HBr the same behaviour is observed as found above in the flow-cell experiment. The anodic dissolution here also starts at

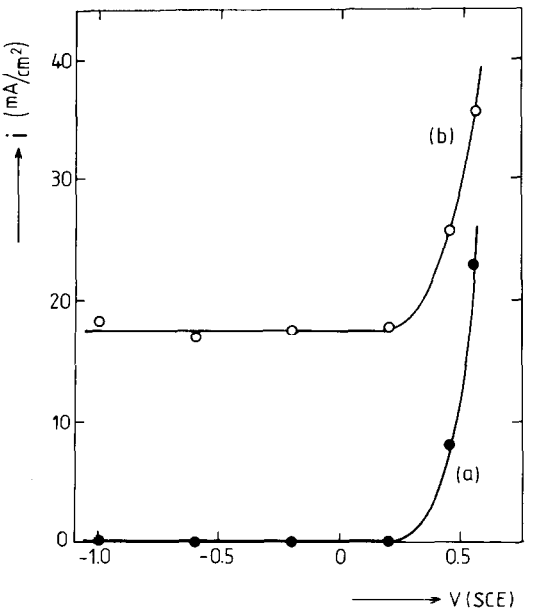

Fig. 3. Flow-cell experiments at a p-InP electrode in the dark in a solution of 0.1M Br_2 and 4.5M HBr. The current–potential curve (a) and the chemical etch rate (b) were measured under potentiostatic control.

about +0.25 V and is shifted 300 mV to negative potentials with respect to the 1N H_2SO_4 solution. The shift in the bromine containing solution is more pronounced than in the HBr solution in curve (b) of this figure.

The log of the chemical etch rate is shown in fig. 4 as a function of the log of the Br_2 concentration in a 4.5M HBr solution for InP crystals with two different orientations. The bromine concentration was varied over almost two orders of magnitude. Curve (a) shows that the slope of the line for the (001) orientation is close to one. This means that the etch rate is first order in bromine concentration. This in turn means that the etch rate can either be kinetically controlled or diffusion controlled. Curve (b) shows the dependence found for InP with the (111) In orientation. The slope is close to 0.5, which means that the etch rate must be kinetically controlled and depends on the square root of the Br_2 concentration.

In order to investigate whether the dissolution of InP(001) is under kinetic of diffusion control the etch rate was measured as a function of the electrode rotation rate. In this experiment the flow-cell was not used, instead an InP(001) rotating disc electrode was etched for 10 min at a constant electrode rotation rate. For each rotation rate a freshly prepared solution (15 ml) was used. Afterwards the indium concentration in each solution was determined

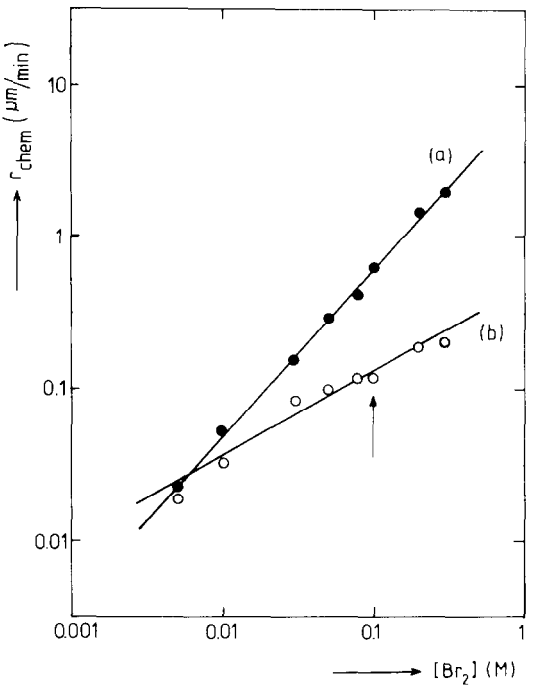

Fig. 4. Chemical etch rate as a function of the Br_2 concentration in a solution of 4.5M HBr is measured with the flow-cell, at p-InP with the (001) surface orientation (a) and the (111) In orientation (b).

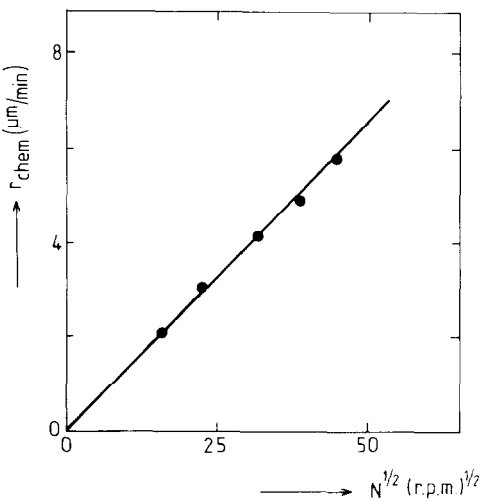

Fig. 5. Chemical etch rate in the dark as a function of the square root of the rotation rate ($N^{1/2}$) of a p-InP(001) electrode in a solution of 0.1M Br_2 and 4.5M HBr.

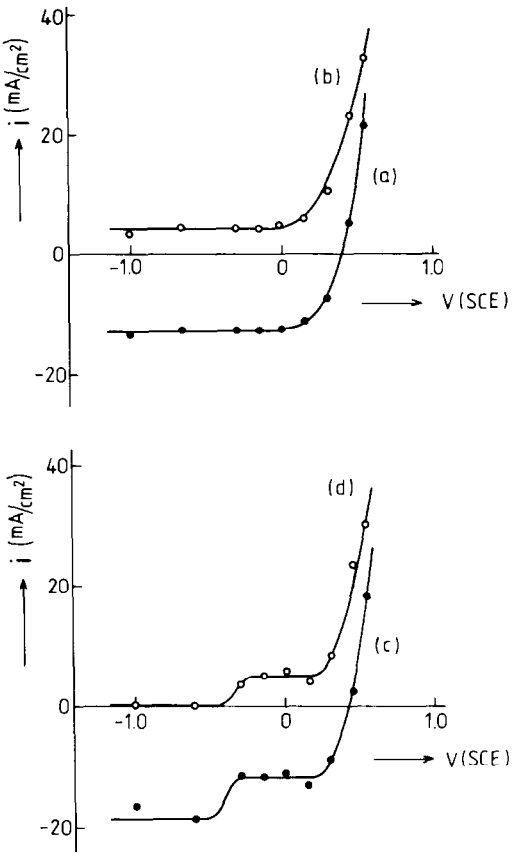

Fig. 6. Flow-cell experiments at a p-InP electrode under illumination in the same solution as used for fig. 3. A moderate light intensity was used for curves (a) and (b) and a high intensity for curves (c) and (d). The current–potential curves (a) and (c) and the chemical rates (b) and (d) were measured under potentiostatic control.

analytically (ICP). Fig. 5 shows the chemical etch rate as a function of the square root of the electrode rotation rate for a p-InP(001) electrode in the dark. A straight line passing through the origin is found. This means that the Levich equation is obeyed and that the chemical etch rate is diffusion-controlled.

So far we have presented results obtained only in the dark. In fig. 6 flow-cell experiments under illumination are shown. The experimental conditions are the same as those described for the dark experiment in fig. 3. In fig. 6 two different light intensities were used. For curves (a) and (b) a moderate light intensity was used. It reveals a large potential independent reduction

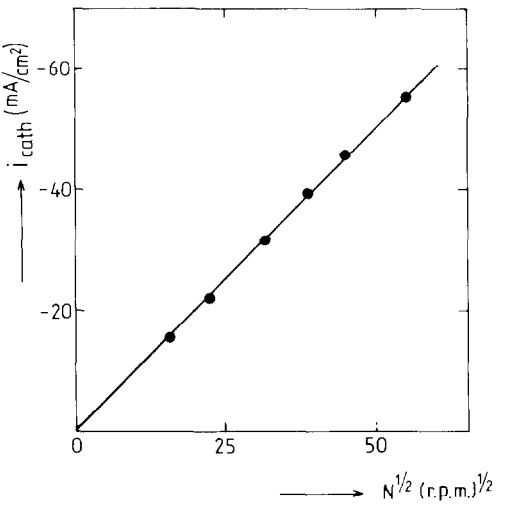

Fig. 7. Plateau current density at a potential of +0.15 V as a function of the square root of the electrode potential for a p-InP(001) rotating disc electrode under illumination with a high light intensity.

current over a broad potential range (curve (a)). In this potential range no hydrogen evolution is observed and the chemical etch rate is reduced to a potential independent value of 4 mA/cm^2 (curve (b)) with respect to the 17.5 mA/cm^2 in the dark case (see curve (b) of fig. 3). As in the dark case at about 0.2 V the current density increases and anodic dissolution of InP starts. Consequently the total etch rate increases at positive potentials (curve (b)). In the lower part of fig. 6 the electrode was illuminated with a higher light intensity. Curves (c) and (d) correspond to the potentiostatically measured current density and chemical etch rate, respectively. The results at potentials more positive than −0.3 V are essentially the same as those found at the lower light intensity. However at potentials more negative than −0.3 V the reduction current in curve (c) increases to a higher value and hydrogen evolution occurs. Due to this gas evolution the reduction fluctuates to some extent. It is clear from curve (d) that in this potential range the chemical etch rate is reduced to zero.

In fig. 7 the dependence of the cathodic current density on the electrode rotation rate is shown for a p-InP(001) rotating disc electrode. The working electrode was illuminated with a high light intensity at a potential of +0.15 V. Thus, the experimental conditions are the same as at the cathodic plateau in the flow-cell experiment of fig. 6 curve (c). The straight line through the origin indicates that the reduction is diffusion-controlled.

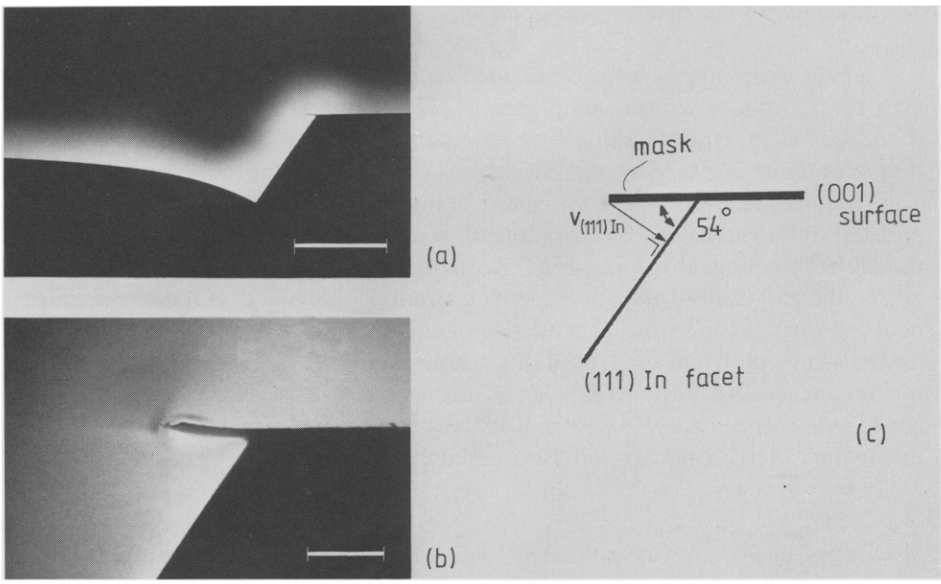

Fig. 8. Etching profile of a p-InP(001) crystal in the dark in a solution of 0.1M Br_2 and 4.5M HBr at two different magnifications, 2500× (a) and 20000× (b). In (a) one bar represents 10 μm and in (b) 1 μm. Etching time was 7.5 min and the temperature was 20 °C. The etch rate of the (111) In plane is defined in (c).

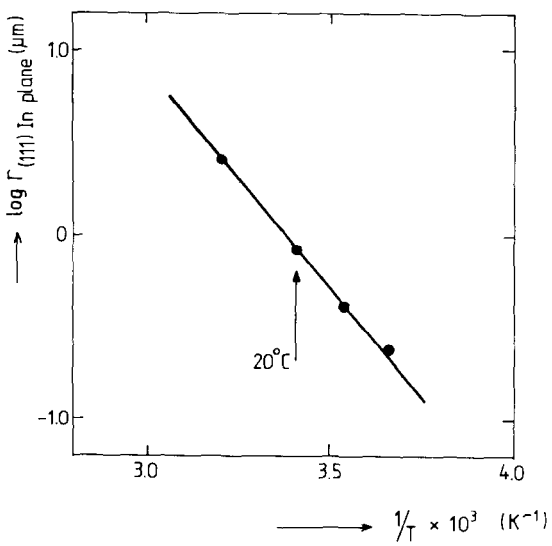

Fig. 9. Logarithm of the etch rate of the (111) In plane, obtained from etching experiments, as a function of the reciprocal temperature. Etching time was 7.5 min.

3.3. Etching profiles in Br_2/HBr solutions

Etching experiments were performed in a solution of 0.1M Br_2 and 4.5M HBr for 7.5 min at various temperatures. The temperature range was between 0 and 40 °C. A typical example of an etching profile is shown in fig. 8 for a temperature of 20 °C. Two magnifications are given of the same profile in (a) and (b). An angle of 54° is measured between the plane near the resist edge and the (001) surface of the InP crystal. Since the SiO_2 mask is orientated in the ($\bar{1}10$) direction, this facet must be attributed to the (111) In plane [4]. We define the etch rate of this facet as the normal of this plane as indicated in (c) of fig. 8. Fig. 9 shows the dependence of this etch rate on the temperature in an Arrhenius plot. The logarithm of the etch rate of the (111) In plane is found to be linear with the reciprocal of the temperature. From the slope an activation energy of 10.7 kcal/mol is calculated. The same etching results as in the dark were obtained under illumination with a high light intensity.

4. Discussion

We shall first discuss the results obtained with HBr solutions. As fig. 1 curve (a) reveals the etch rate of InP is strongly dependent on the HBr content. The etch rate is very low at concentrations lower than 5 molar. This result is similar to that found in earlier work for InP in HCl solutions [11]. There we argued that HCl acts as a chemical etchant and that HCl molecules are needed to dissolve InP. In the present case it is also clear that HBr molecules are needed to dissolve InP; since HBr is a very strong acid in aqueous solutions ($k_a = 10^{+6}$ [14]) dissociation is complete at HBr concentrations lower than 5 molar, and no etching occurs. Only at high concentrations the degree of dissociation is lower as a result of water deficiency and InP is etched by HBr molecules. This is confirmed in curve (b) of fig. 1 where HBr is diluted with acetic acid. In this environment HBr becomes a weak acid ($k_a = 10^{-7}$ [15a,b]). Thus the degree of dissociation in acetic acid solutions is negligible even at low concentrations and a linear relationship, with high etch rates compared to aqueous HBr solutions, is expected. This suggests that HBr, like HCl acts as a chemical etchant. This is also expressed in the current–potential curve of fig. 2 curve (b) where the anodic dissolution of InP starts 150 mV earlier in 4.5M HBr than in a solution of 1N H_2SO_4, i.e. the activation energy for the electrochemical dissolution is lowered by the chemical etchant. This can be explained when the first rate-determining step in the anodic dissolution of InP is replaced by a chemical dissolution step, the remaining bonds are then more easily attacked anodically. In conclusion we may say that InP is etched chemically by HBr molecules. The mechanism of the chemical dissolution of semiconductors is proposed before for symmetric

[16] and asymmetric [11] chemical etchants. For HBr, also a bifunctional asymmetric molecule, the first step in the chemical dissolution of InP can be described by a synchronous exchange of bonds according to

(3)

Two more HBr molecules are needed to remove an In and a P atom from the crystal lattice as hydrolysed $InCl_3$ and PH_3 as gas. We indeed observed in the experiments that gas is evolved during dissolution of InP in HBr solutions.

We now consider solutions of 4.5M HBr containing bromine. The etch rate in 4.5M HBr can be neglected (see fig. 1 curve (a)). So etching results in solutions of Br_2 in 4.5M HBr must be attributed to Br_2. From the potential independent etch rate in the flow-cell experiment of fig. 3 in a solution of 0.1M Br_2/4.5M HBr we already concluded that InP is etched chemically. This must be attributed to complexed Br_2 in the solution only. That InP is etched chemically by Br_2 can also be clearly seen in curve (c) of fig. 2. Here the shift of the anodic dissolution curve is even more pronounced due to a much higher etch rate than in 4.5M HBr. The explanation of this shift is the same as given above for HBr solutions. The mechanism of the chemical dissolution of InP by a symmetric Br_2 molecules can be represented in the same way as Gerisher and Wallem-Mattes [16] proposed for GaAs, as

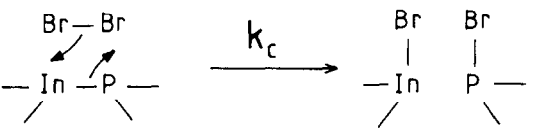

(4)

where k_c is the rate constant of the first rate-determining step in the dissolution process. Again, to dissolve one InP entity, two more Br_2 molecules are needed. From the Levich dependence in fig. 5 and the etch rate dependence on the Br_2 concentration (curve (a) of fig. 4) we must conclude that the chemical dissolution rate is controlled by Br_2 diffusion in the solution and thus that k_c is large. This holds for InP with a (001) orientation. For InP with a (111) In surface the etch rates are significantly lower (curve (b) of fig. 4). The etch rate is here kinetically controlled. From the slope of this figure a reaction order of 0.5 is observed which implies that one bromine atom is involved in the rate-determining dissolution step. This would mean that in this case no simultaneous exchange of bonds occurs. A possible explanation would be that due to steric hindrance a bromine molecule cannot attack In and P atoms simultaneously. From a crystallographic point of view the P atoms are deeply hidden behind the In atoms of the (111) In surface and can therefore not be approached easily by a large molecule such as Br_3^-.

The electrochemical results of fig. 6 under illumination indicate that Br_2 is reduced at negative potentials (curves (a) and (c)) according to

$$Br_2 + 2\ e \xrightarrow{k_e} 2\ Br^-. \tag{5}$$

From these results it is not clear whether the reduction takes place via simple conduction band process or a mixed conduction band/valence band process [12,19]. It should be noted that it is not easy to distinguish the two cases as van den Meerakker showed for the reduction of I_2 at p-GaAs [12]. In this work, however, it is not important to discriminate between the two reactions. When the photon flux is high the Br_2 reduction is diffusion-controlled as the Levich dependence of fig. 7 shows. This means that k_e is large. Due to this high photon flux an excess of photoelectrons are created which recombine with holes at potentials more positive than -0.6 V in curve (c) of fig. 6. Recombination stops at potentials negative with respect to -0.6 V and hydrogen is evolved in addition to the Br_2 reduction. This also indicates that the light intensity used in curve (a) of this figure is critical since the rate of Br_2 reduction is the same as in curve (c) and the current does not increase at cathodic potentials; here no hydrogen is evolved. Due to the electrochemical reduction of Br_2 the chemical etch rate of InP is reduced dramatically (compare fig. 3 curve (b) with fig. 6 curve (b) and (d)). Similar results have been found for the reduction of hypochlorite at p-GaAs [13]. However since the Br_2 reduction is diffusion-controlled it is remarkable that the etch rate is not zero. This behaviour can only be explained as follows: both k_c and k_e are large, so the reaction rate of each reaction is determined by Br_2 diffusion in the solution. The ratio of the k's can be deduced from the ratio of the chemical etch rate (curve (a)) and reduction rate (curve (b)). It follows that

$$k_e/k_c \simeq 3. \tag{6}$$

The two values must be similar in magnitude. The k's and thus the ratio of k's are independent of the electrode rotation rate. Then it is possible that the Levich equation is obeyed for both processes at the same time, while the total Br_2 consumption is, of course, diffusion-controlled. Note that the sum of the chemical etch rate and the Br_2 reduction rate under illumination in fig. 6 is exactly that for the chemical etch rate in the dark alone (see fig. 3). Moreover, the diffusion-coefficient of Br_3^- which can be calculated from the Levich dependences for the chemical dissolution reaction and the electrochemical reduction reaction in figs. 5 and 7, respectively, are exactly the same as one would expect for one species ($\mathscr{D}_{Br_3^-} = 1.0 \times 10^{-5}$ cm^2/s).

In curve (d) of fig. 6 it is found that the chemical etch rate is decreased to zero in the potential range where hydrogen is evolved. Gagnaire et al. [17] described the cathodic decomposition of InP in alkaline solutions as a result of hydrogen evolution. An indium-rich surface is then formed. We propose that

in acid solutions the same cathodic decomposition occurs which prevents Br_2 from etching the InP surface at a significant rate. The importance of hydrogen for the decomposition of InP is clearly shown in curve (b) of fig. 6 where the chemical etch rate does not decrease when hydrogen evolution is absent.

The electrochemical results obtained in Br_2/HBr solutions are strongly related to the shape of etched profiles. In refs. [6,7] it is mathematically deduced and experimentally confirmed that round profiles near resist edges are obtained when the dissolution rate of all crystal planes is diffusion-controlled. The importance of the mechanism of the dissolution reaction was studied in detail in refs. [7,8]. The conclusion was that round profiles near the resist edge are obtained only in a special case with electrochemical etchants [8] and in general with diffusion-controlled chemical etchants. In the present paper we discussed that we are dealing with Br_2 as chemical etchant but that the etch rate is not diffusion-controlled at all crystal planes. So, in this case, we may not expect round profiles. Indeed, the etched profile of fig. 8 shows the (111) In facet near the resist edge, the same facet which macroscopically was found to be kinetically controlled. An activation energy of 10.7 kcal/mol, typical for kinetic controlled processes [18], found in the Arrhenius plot of fig. 9, confirms this. The agreement of the etch rate of the (111) In facet in the etched profiles and the macroscopic etch rate of this plane is striking (compare arrows in fig. 4 and fig. 9). From the electrochemical results under illumination it is not possible to predict under which mechanism InP is etched at the rest potential.

Acknowledgements

The authors with to thank the Analytical Department of Ir. P.J. Rommers for the indium analyses, Mr. C. Geenen for making the SEM photographs and Prof. Dr. J.J. Kelly and Mr. J.E.A.M. van den Meerakker for helpful discussions.

References

[1] A. Guivarc'h, H. L'Haridon, G. Pelous, G. Hollinger and P. Pertosa, J. Appl. Phys. 55 (1984) 1139.
[2] Y. Nishitani and T. Kotani, J. Electrochem. Soc. 126 (1979) 2269.
[3] Y. Tarni, Y. Komiya and Y. Harada, J. Electrochem. Soc. 118 (1971) 118.
[4] S. Adachi and H. Kawaguchi, J. Electrochem. Soc. 128 (1981) 1342.
[5] Gmelins Handbuch der Anorganischen Chemie, Brom (7) (Verlag Chemie, Berlin, 1931), p. 115.
[6] H.K. Kuiken, J.J. Kelly and P.H.L. Notten, J. Electrochem. Soc. 133 (1986) 1217.
[7] P.H.L. Notten, J.J. Kelly and H.K. Kuiken, J. Electrochem. Soc. 133 (1986) 1226.
[8] P.H.L. Notten and J.J. Kelly, J. Electrochem. Soc. 134 (1987) 444.

[9] C.J. Keavney and H.I. Smith, J. Electrochem. Soc. 131 (1984) 452.
[10] E. Haroutiounian, J. Sandino, P. Clechet, D. Lamouche and J. Martin, J. Electrochem. Soc. 131 (1984) 27.
[11] P.H.L. Notten, J. Electrochem. Soc. 131 (1984) 2641.
[12] J.E.A.M. van den Meerakker, Electrochim. Acta 30 (1985) 435.
[13] P.H.L. Notten, J. Electroanal. Chem., in press.
[14] W. Huber, Titrations in Nonaqueous Solvents (Academic Press, New York, 1967) p. 215.
[15] (a) I. Gyenes, Titration in Non-Aqueous Media (Iliffe Books, London, 1967) p. 39.
(b) See ref. [14], p. 226.
[16] H. Gerisher and I. Wallem-Mattes, Z. Phys. Chem. (NF) 64 (1969) 187.
[17] A. Gagnaire, J. Joseph, A. Etcheberry and J. Gautron, J. Electrochem. Soc. 132 (1985) 1655.
[18] Y. Mori and N. Watanabe, J. Electrochem. Soc. 125 (1978) 1510.
[19] H. Gerisher, Surface Sci. 18 (1969) 97.